COMMUNICATIONS IN COMPUTATIONAL PHYSICS
Vol. **5**, No. 2-4, pp. 667-682

Commun. Comput. Phys.
February 2009

p-Multigrid Method for Fekete-Gauss Spectral Element Approximations of Elliptic Problems

Richard Pasquetti* and Francesca Rapetti

Laboratoire J.A. Dieudonné, UMR 6621 CNRS, Université de Nice Sophia-Antipolis, Parc Valrose, 06108 Nice cedex 02, France.

Received 28 September 2007; Accepted (in revised version) 8 January 2008

Available online 1 August 2008

Abstract. An efficient p-multigrid method is developed to solve the algebraic systems which result from the approximation of elliptic problems with the so-called Fekete-Gauss Spectral Element Method, which makes use of the Fekete points of the triangle as interpolation points and of the Gauss points as quadrature points. A multigrid strategy is defined by comparison of different prolongation/restriction operators and coarse grid algebraic systems. The efficiency and robustness of the approach, with respect to the type of boundary condition and to the structured/unstructured nature of the mesh, are highlighted through numerical examples.

AMS subject classifications: 65N30, 65N35, 65N55

Key words: Spectral elements, Fekete points, multigrid methods.

1 Introduction

The Spectral Element Method (SEM), developed in the 80's to solve with spectral-like methods Partial Differential Equations (PDE) in non-Cartesian (non-cylindrical, non-spherical,$\cdots$) geometries, has proved to be very successful during the two last decades, see, *e.g.*, [8, 16]. Its main drawback is however to be not really adapted to very complex geometries, due to the non-simplicial shape of the elements which are the image of the cube $\hat{\Omega}=(-1,1)^d$, where d is the space dimension, in which the polynomial approximation holds.

Some ways have been suggested to support triangular/tetrahedral elements and hence simplicial meshes. Among them is the one proposed in [16], which makes use of the "collapsed coordinate system" resulting from a singular mapping from the

*Corresponding author. *Email addresses:* richard.pasquetti@unice.fr (R. Pasquetti), francesca.rapetti@unice.fr (F. Rapetti)

2D/3D cube onto the triangle/tetrahedron. This approach has appeared of great interest, but suffers from a non-symmetric distribution of the interpolation points in the triangle/tetrahedron, with an useless accumulation of these points in one of the vertices.

The SEM being a nodal method, *i.e.*, the basis functions are Lagrange polynomials based on interpolation points, the main research axis was then to provide points in the simplex showing nice interpolation properties, *i.e.*, such that the Lebesgue constant does not increase fastly with the degree of the polynomial approximation, see, *e.g.*, [4,5,13,14]. Here we are interested in Fekete points based methods, as proposed for the triangle in [27], due to their nice interpolation properties and strong link with the Gauss-Lobatto Legendre (GLL) nodes of the quadrangle based SEM, say *Q*SEM, since Fekete points and GLL points coincide in the d-dimensional cube [2].

In contrast to the GLL points, the Fekete points are however not Gauss points, so results obtained with the earlier triangle based SEM, say *T*SEM, proposed in [28] may be disappointing. High-accuracy quadrature rules are indeed needed to preserve the "spectral accuracy" of SEM type methods, which are based on variational formulations. This has motivated new researches, to find a unique set of points with nice interpolation and quadrature properties [29, 30] or at least to develop more sophisticated quadrature rules [31]. Such researches are not yet satisfactory. Thus, the quadrature rule of [31] is costly and requires a linear mapping from the reference triangle T to the spectral element; if the mapping is non-linear, then a quadrature rule specific to each element must be set up [15]. For us we have proposed to consider the Gauss points of the triangle as quadrature points and the Fekete points as interpolation points, in the frame of a "Fekete-Gauss *T*SEM" [20].

Once the approximation procedure is fixed it remains to develop efficient solvers for the associated algebraic systems. As well known, the matrices resulting from high order approximations are indeed ill-conditioned, with $\mathcal{O}(N^4)$ condition numbers in 2D, where $N \equiv p$ is the total degree of the polynomial approximation in each spectral element. We thus have focused on domain decomposition techniques, each spectral element being considered as a subdomain. The following methods have been considered:

- Neumann-Neumann Schur complement methods [21]: Addressing the Schur complement with Neumann-Neumann type preconditioners has yielded promising results. Moreover, the condition number of the Schur complement only shows a $\mathcal{O}(N)$ behavior.
- Overlapping Schwarz methods [22]: Impressive results can be obtained but with the drawback that, in contrast to the *Q*SEM, a "generous overlap" (overlap of one entire mesh element) must be used due to the non-tensorial distribution of the Fekete points in the element.

In parallel, it was of interest to revisit the p-multigrid approach, which makes use of a fixed simplicial mesh and of different approximation levels, each of them associated with a different polynomial degree. For the *Q*SEM this was initially suggested in [18, 23, 24] and recently used in conjunction with Overlapping Schwarz preconditioners for

Computational Fluid Dynamics (CFD) purposes in [11]. Of course, results have also been achieved in the frame of standard spectral methods [12, 33] or in the frame of *hp*-finite elements, see, *e.g.*, [17, 19], and the basics of multigrid methods may be found in famous books, see [3, 32] and references herein. Preliminary results of *p*-multigrid methods for the *T*SEM were presented in [9].

The paper is organized as follows. In Section 2 we briefly recall some basic elements of the Fekete-Gauss *T*SEM, see the "TSEM-3" approach of [20] for more details. In Section 3, we consider the single triangle case and check different strategies to set up the prolongation and restriction matrices as well as the coarse grid algebraic systems. The study is carried out for second order elliptic problems and extends the one given in [9]. Once a strategy has been fixed we go to real spectral element discretizations, in Section 4, and focus on the robustness of the method with respect to the mesh and to the type of boundary condition. We conclude in Section 5.

2 The Fekete-Gauss TSEM

The *Q*SEM makes use of the GLL points for both the interpolation and the quadrature points: GLL points indeed have nice approximation and integration properties. Such a single set of points does not exist for the triangle. Consequently, the Fekete-Gauss *T*SEM makes use of two sets of points:

• The Fekete points, as interpolation points.

Let $T=\{(r,s):\ -1\leq r,s,\ r+s\leq 0\}$ be the reference triangle and $\mathcal{P}_N(T)$ the set of real polynomials on T of total degree $\leq N$. Let $n=(N+1)(N+2)/2$ be the dimension of $\mathcal{P}_N(T)$ and $\{\psi_j\}_{j=1}^n$ any basis of $\mathcal{P}_N(T)$. The Fekete points $\{x_i\}_{i=1}^n$ are those which maximize over T the determinant of the Vandermonde matrix V, such that $V_{ij}=\psi_j(x_i)$, $1\leq i,j\leq n$.

Some nice properties of the Fekete points are the following [1, 2, 27]: (i) The Lagrange polynomials, say $\{\varphi_i(x)\}_{i=1}^n$, based on the Fekete points achieve maximum at these points; (ii) Fekete points are GLL points for the cube; (iii) On the sides of the triangle the Fekete points coincide with the GLL points. This result has an important application: Fekete point triangular elements naturally conform with standard quadrilateral spectral elements.

With u_N for the spectral element approximation of u we then write:

$$u(x)\approx u_N(x)=\sum_{i=0}^{n} u_N(x_i)\,\varphi_i(x),\quad x\in T. \tag{2.1}$$

• Gauss points, as quadrature points.

The determination of the Gauss points of the triangle is not a trivial task and so has motivated a lot of researches [26]. Of course, it is possible to start from the Gauss points of the square and to use a mapping from the quadrangle onto the triangle [16, 25], but to achieve an exact integration, say in $\mathcal{P}_M(T)$ with $M\approx 2N$ and $m\approx n$ quadrature points, it

is better to look for a symmetric distribution of the Gauss points. Recent results on this topic may be found in [6]. Then:

$$\int_T v dT \approx \int_T v_M dT = \sum_{i=0}^{m} \rho_i v_M(y_i), \tag{2.2}$$

where the y_i and ρ_i are the Gauss quadrature points and weights, respectively, see, *e.g.*, [7].

The Fekete-Gauss *T*SEM shows some advantages:

- Just like the *Q*SEM, the Fekete-Gauss *T*SEM makes use of a highly accurate quadrature rule. Moreover, this may be done in a flexible way, *i.e.*, exact integration in $\mathcal{P}_{2N-q}$, $q=0,1,\cdots$.
- Differentiation matrices allow to compute derivatives at the Gauss points from the Fekete point values: no interpolations are needed to compute the stiffness matrix.
- Non-linear mappings (curved triangles) are easily supported.

However, some drawbacks with respect to *Q*SEM should be mentioned:

- The mass matrix is not diagonal. This is especially a drawback in the frame of evolution problems when using an explicit scheme for the time integration.
- Differentiation matrices are n-dimensional rather than $(N+1)$. This fact is true for any non-tensorial arrangement of the grid-points (price of unstructured meshes).
- The resulting algebraic system matrix, say A, is ill-conditioned: The condition number of A shows an $\mathcal{O}(N^4)$ behavior in 2D, with respect to $\mathcal{O}(N^3)$ for the *Q*SEM.

3 Multigrid strategy

The goal of this Section is to develop a p-multigrid strategy, *i.e.*, to define the prolongation/restriction operators between different approximation levels, an efficient way to set up the coarse grid algebraic systems and the smoothing procedure. This is done by considering only one triangular spectral element. We address here the two grid-case, but the approach can be easily extended to an arbitrary number of grids. For the sake of simplicity we use the term grid to denote the set of Fekete points $\{x_i\}_{i=1}^{n} \in T$ associated with a given approximation polynomial degree N over T.

The superscripts c and f are hereafter used to denote the coarse and fine grids, respectively associated with a low and a high polynomial degree. Thus, for the coarse grid N_c is the polynomial approximation degree, $\{x_i^c\}_{i=1}^{n_c}$ the set of Fekete points and $\{\varphi_i^c\}_{i=1}^{n_c}$ the corresponding Lagrange polynomials. Accordingly, for the fine grid we use N_f, $\{x_i^f\}_{i=1}^{n_f}$ and $\{\varphi_i^f\}_{i=1}^{n_f}$, with $N_f > N_c$.

In the frame of spectral methods, defining the prolongation operator is quite natural. Using the polynomial interpolant yields:

$$u_f(x_i^f)=\sum_{j=1}^{n_c} u_c(x_j^c)\varphi_j^c(x_i^f), \quad 1\le i\le n_f, \tag{3.1}$$

where u_c (u_f) denotes u_{N_c} (u_{N_f}). In matrix notation we thus obtain the prolongation operator P, such that:

$$\boldsymbol{u}_f = P\boldsymbol{u}_c, \quad [P]_{ij}=\varphi_j^c(x_i^f). \tag{3.2}$$

Note that the side point values of $\boldsymbol{u}_f$ only depend on the side point values of $\boldsymbol{u}_c$. There are indeed $N+1$ Fekete points on each side of T, so that the Lagrange polynomials based on points on the other sides or inside T vanish at this side. As a result, the operator P shows a special structure. Thus, if the boundary points are arranged before the inner points:

$$P=\begin{pmatrix} P_{BB} & 0 \\ P_{IB} & P_{II} \end{pmatrix}, \tag{3.3}$$

where the subscripts B and I are used for boundary and inner points, respectively. Operator P is a $n_f\times n_c$ matrix whereas P_{BB} is a $3N_f\times 3N_c$ block. In the multigrid context, the prolongation operator extends a coarse grid error $\boldsymbol{e}_c$ to obtain a fine grid correction $\boldsymbol{e}_f = P\boldsymbol{e}_c$. Thus, the side point values of $\boldsymbol{e}_f$ only depend on the side point values of $\boldsymbol{e}_c$.

Defining the restriction operator, say R, is less trivial. As just done for the prolongation operator, one may proceed by *interpolation* to obtain:

$$u_c(x_i^c)=\sum_{j=1}^{n_f} u_f(x_j^f)\varphi_j^f(x_i^c), \quad \boldsymbol{u}_c = R\boldsymbol{u}_f, \quad [R]_{ij}=\varphi_j^f(x_i^c). \tag{3.4}$$

A clever handling of the highest frequencies cannot really be expected from the interpolation strategy and one may then prefer to proceed by *projection* or more generally by *filtering*. To this end, let $\{\psi_i\}_{i=1}^{\infty}$ be an orthogonal hierarchical basis over the triangle T, *e.g.*, the Koornwinder-Dubiner basis [10], then:

$$u_f(x)=\sum_{j=1}^{n_f}\hat{u}_j\psi_j(x) \quad \textit{and} \quad u_c(x_i^c)=\sum_{j=1}^{n_f} Q_j\hat{u}_j\psi_j(x_i^c), \tag{3.5}$$

so that: $R=\tilde{V}_c Q {V_f}^{-1}$. Here, V_f is the previously defined Vandermonde matrix for the fine grid and $\tilde{V}_c$ the $n_c\times n_f$ matrix such that $[\tilde{V}_c]_{ij}=\psi_j(x_i^c)$, *i.e.*, an extension of the coarse grid Vandermonde matrix V_c. The matrix Q is diagonal of dimension $n_f\times n_f$, with the Q_j for elements. For a projection one simply has $Q_j=1$ if $j\le n_c$ and $Q_j=0$ if $n_c<j\le n_f$. For a filtering, the values of the Q_j should be associated with the total degree of the polynomial ψ_j, say $N(j)$. Using, *e.g.*, the raised cosine filter $Q_j=(\cos(N(j)/N_f)\pi)+1)/2$.

In the frame of variational methods, weak formulations with $L^2(T)$ inner products are involved. Taking that into account yields to set up a restriction operator by *transposition* of the prolongation operator. Indeed,

$$(u_f,\varphi_i^c)=(u_f,\sum_{j=1}^{n_f}\varphi_i^c(x_j^f)\varphi_j^f)=\sum_{j=1}^{n_f}\varphi_i^c(x_j^f)(u_f,\varphi_j^f), \tag{3.6}$$

so that $R=P^t$.

In the context of a multigrid method, the restriction operator acts on a residual at the fine grid level, $\boldsymbol{r}_f$, to obtain a vector $\boldsymbol{b}_c=R\boldsymbol{r}_f$ at the coarse grid level. If R is obtained by interpolation, then it shows a structure similar to P. If R is obtained by projection, then it does not show any special structure. Finally, if R is obtained by transposition of P, then its structure is such that the inner point values of $\boldsymbol{b}_c$ only depend on the inner point values of $\boldsymbol{r}_f$.

Once the prolongation and restriction operators have been fixed, it remains to set up the coarse grid matrix, say A_c.

Matrix A_c may be set up *directly*, *i.e.*, like the fine grid level matrix A. This approach was the one used in the earlier paper [23].

Matrix A_c may also be set up by *aggregation* of A: $A_c=RAP$. Note that this must be done with the elemental matrices, *i.e.*, before stiffness summation, if more than one element is considered, or before taking care of the boundary conditions. Concerning the boundary conditions at the coarse grid level, or more generally at all sublevels if more than two grid levels are considered, they must be taken homogeneous and of the same type, Dirichlet, Neumann or Robin, involved in the initial problem.

The aggregation approach is generally coupled to the definition of the restriction operator by transposition. One can indeed easily check that: If $A_c=RAP$ and $R=P^t$, and if A is symmetric and positive definite, then $\boldsymbol{e}_c$ such that $A_c\boldsymbol{e}_c=R\boldsymbol{r}_f$ solves the constrained optimization problem: Minimize

$$\begin{aligned}&\phi(\boldsymbol{u}^*)=\frac{1}{2}(A\boldsymbol{u}^*,\boldsymbol{u}^*)-(\boldsymbol{b},\boldsymbol{u}^*)\quad \textit{constrained by}\\ &\boldsymbol{u}^*=\boldsymbol{u}_f+P\boldsymbol{e}_c.\end{aligned} \tag{3.7}$$

First one notices that, since $A=A^t$, any solution of the non-constrained problem solves $A\boldsymbol{u}^*=\boldsymbol{b}$, *i.e.*, $\boldsymbol{u}^*$ solves the fine grid level system. If one replaces $\boldsymbol{u}^*$ with $\boldsymbol{u}_f+P\boldsymbol{e}_c$, after some simple manipulations we obtain:

$$\phi(\boldsymbol{u}_f+P\boldsymbol{e}_c)\equiv\hat{\phi}(\boldsymbol{e}_c)=\frac{1}{2}(P^tAP\boldsymbol{e}_c,\boldsymbol{e}_c)+(P^tA\boldsymbol{u}_f,\boldsymbol{e}_c)-(P^t\boldsymbol{b},\boldsymbol{e}_c)+Cte.$$

Now we compute the gradient of $\hat{\phi}(\boldsymbol{e}_c)$ and equal it to 0. This yields:

$$P^t(A\boldsymbol{u}_f-\boldsymbol{b})+P^tAP\boldsymbol{e}_c=0.$$

$\boldsymbol{MG(N_c,N_m,N_f)}$
1. *On the fine grid*

Pre-smoothing: $\boldsymbol{u}_f^k = GS(\boldsymbol{u}_f^{k-1},A,\boldsymbol{b}), \quad k=1,\cdots,K.$
$\boldsymbol{u}_f^0 \leftarrow \boldsymbol{u}_f^K.$

Form the residual: $\boldsymbol{r}_f = \boldsymbol{b} - A\boldsymbol{u}_f^0.$

2. *On the middle grid*

Restrict the residual: $\boldsymbol{b}_m = R_f^m \boldsymbol{r}_f.$

Pre-smoothing: $\boldsymbol{e}_m^k = GS(\boldsymbol{e}_m^{k-1},A_m,\boldsymbol{b}_m), \quad k=1,\cdots,K.$
$\boldsymbol{e}_m^0 \leftarrow \boldsymbol{e}_m^K.$

Form the residual: $\boldsymbol{r}_m \leftarrow \boldsymbol{b}_m - A_m\boldsymbol{e}_m^0.$

3. *On the coarse grid*

Restrict the residual: $\boldsymbol{b}_c = R_m^c \boldsymbol{r}_m.$
Solve the residual problem: $A_c\boldsymbol{e}_c = \boldsymbol{b}_c.$

4. *On the middle grid*

Correct the solution: $\boldsymbol{e}_m^0 \leftarrow \boldsymbol{e}_m^0 + P_c^m \boldsymbol{e}_c.$

Post-smoothing: $\boldsymbol{e}_m^k = GS(\boldsymbol{e}_m^{k-1},A_m,\boldsymbol{b}_m), \quad k=1,\cdots,K.$
$\boldsymbol{e}_m^0 \leftarrow \boldsymbol{e}_m^K.$

5. *On the fine grid*

Correct the solution: $\boldsymbol{u}_f^0 \leftarrow \boldsymbol{u}_f^0 + P_m^f \boldsymbol{e}_m^0.$

Post-smoothing: $\boldsymbol{u}_f^k = GS(\boldsymbol{u}_f^{k-1},A,\boldsymbol{b}), \quad k=1,\cdots,4.$
$\boldsymbol{u}_f^0 \leftarrow \boldsymbol{u}_f^K$

Figure 1: The above algorithm describes one V-cycle of a p-multigrid procedure based on three levels, say $MG(N_c,N_m,N_f)$. In this case one has two restriction operators, from the fine grid to the middle one, R_f^m, and from the middle grid to the coarse one, R_m^c. Similarly one has two prolongation operator, P_c^m and P_m^f. "GS" means here one sweep Gauss-Seidel smoothing. Vectors $\boldsymbol{u}_f^0$ and $\boldsymbol{e}_m^0$ are initialized to 0. The integer K denotes the number of GS iterations, *i.e.*, $K=4$ in the present numerical experiments.

Taking into account $P^t = R$ and $\boldsymbol{b} - A\boldsymbol{u}_f = \boldsymbol{r}_f$ yields the desired result:

$$A_c\boldsymbol{e}_c = R\boldsymbol{r}_f, \quad A_c = RAP.$$

Single triangle numerical test: Depending on,

- the restriction strategy: *Interpolation (I)*, *Transposition (T)*, *Projection (P)* or *Filtering (F)*.
- the coarse matrix set up: *Direct (D)* or *Aggregation (A)*,
  five multigrid strategies have been considered, *I-D, T-D, P-D, F-D* and *T-A*, and compared through a single triangle numerical test.

A multi-level V-cycle is used. For the smoothing at each level, following the study carried out in [9], we simply use 2×4 Gauss-Seidel iterations per grid level, without any relaxation or preconditioning. At the coarsest level, the solution is obtained with an exact solve, the coarsest algebraic system being inverted once for all.

The previous developments can easily be extended to more than 2 grids and the number of grids is arbitrary in our implementation. For the sake of comprehension, in Fig. 1 we describe in detail the adopted p-algorithm in the case where three grids are considered. As before, subscripts f and c refer to the fine and coarse grids, respectively, while m is associated with any middle grid.

Tests for one triangle have been carried out for the elliptic PDE: $-\Delta u+u=f$ in $g(T)$, where g is a given linear mapping, with Dirichlet boundary conditions and a source term f which correspond to the exact solution

$$u_{exact}=\sin(2x+y)\sin(x+1)\sin(1-y).$$

Up to 4 grids have been used. As a matter of example, the set of Fekete points associated with four different polynomial degrees are shown in Fig. 2.

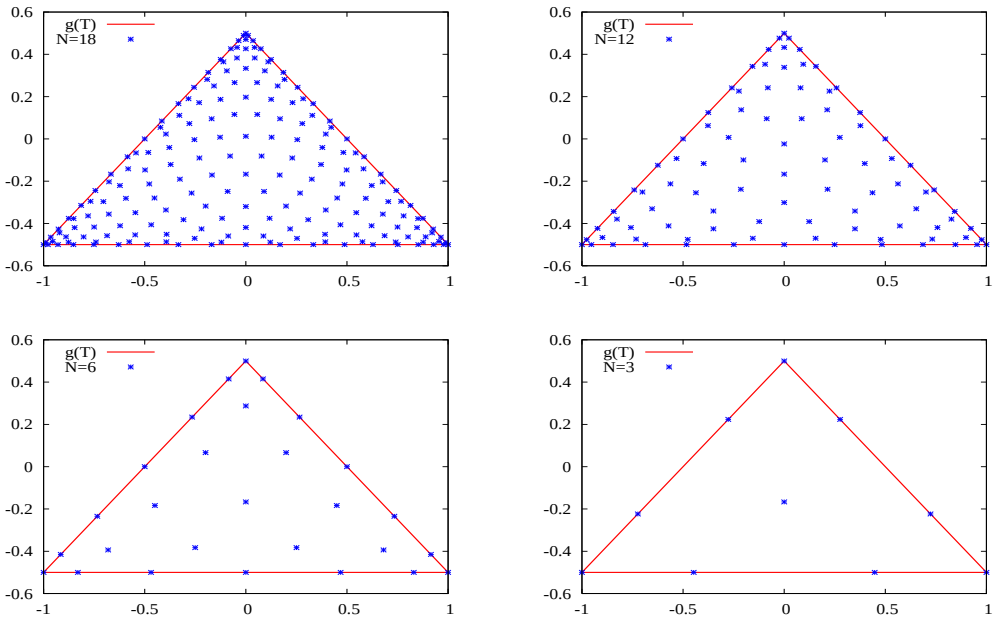

Figure 2: The different grids of the V-cycles.

Results are given in Table 1, where are reported the number of smoothing iterations and the number of V-cycle for each strategy and different grid combinations. Moreover, comparisons are also provided with the standard Gauss-Seidel solution. Note that these results slightly differ from the preliminary ones given in [9], due to the fact that no mapping g was used at this time.

Table 1: Number of iterations at the fine grid level/number of V-cycles to get a residual less than 10^{-6}. Comparisons with Gauss-Seidel (GS) method.

$(N_c,\cdots,N_f)$	*I-D*	*T-D*	*P-D*	*F-D*	*T-A*	GS
(6,12)	76 / 10	36 / 5	80 / 10	80 / 10	36 / 5	101
(3,6,12)	76 / 10	36 / 5	80 / 10	80 / 10	36 / 5	101
(6,12,18)	112 / 14	76 / 10	116 / 15	120 / 15	76 / 10	244
(3,6,12,18)	112 / 14	76 / 10	116 / 15	120 / 15	76 / 10	244

The present single triangle numerical tests yield the following conclusions:

- *I-D*, *P-D* and *F-D* strategies give coherent results. One observes that using the more involved Projection or Filtering strategies does not yield any improvements of the results with respect to Interpolation one.
- *T-D* and *T-A* Strategies give the best results. This could be expected since strategies based on the use of the transpose of the prolongation operator for restriction are well justified for approximations of variational formulations.
- The number of V-cycles and so the number of iterations at the fine grid level depends essentially on N_f and not on the number of levels of the V-cycle. This is especially interesting: Even with a high polynomial approximation degree at the finest grid level, one can think to reach the coarsest (and so the cheapest) one with $N_c=1$ for the direct solve.

4 Numerical tests on simplicial meshes

The *T-D* and *T-A* multigrid strategies, which are well justified both theoretically and from the single triangle numerical tests, have been implemented in a *T*SEM solver of elliptic problems. Since the restriction and prolongation operators do not depend on the mapping from the reference triangle T to the spectral element, the global coarse grid algebraic matrix A_c is first set up by using the usual stiffness summation technique. Thus, if two grids are involved:

$$A_c=\sum_k{}' R A_k P, \qquad R=P^t, \tag{4.1}$$

where $\sum'$ stands for stiffness (assembling) summation and A_k for the elemental matrix associated with the element k. Second, one imposes the boundary conditions to obtain the final form of matrix A_c. As previously mentioned, at the sublevels the boundary conditions are homogeneous and of the type of those of the fine grid level.

The goal is now to check the performances of the present p-multigrid approach, in *T-A* form. As pointed out farther, similar results may be obtained with the *T-D* form. Especially we are interested in its robustness with respect to the boundary conditions,

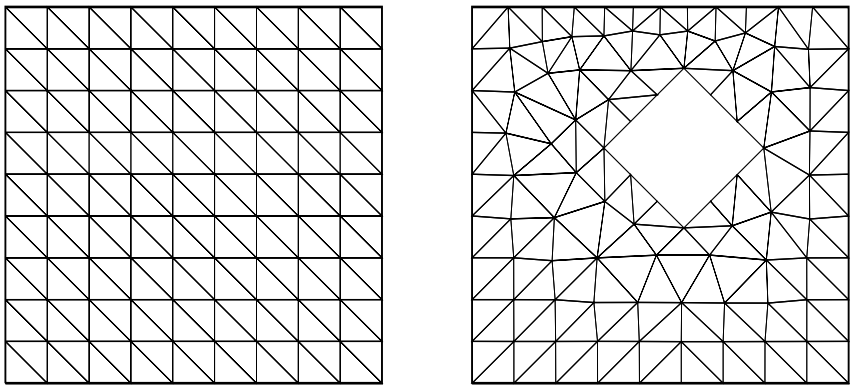

Figure 3: Computational domains and structured and non-structured h-meshes.

Table 2: Number of elements of the structured and non-structured meshes. Corresponding numbers of degrees of freedom (dof) at the fine grid level for different polynomial approximation degrees.

	Structured	non-structured
Number of elements	162	163
$dof(N_f=12)$	11881	12042
$dof(N_f=18)$	26569	26865

to be sure that the performances do not deteriorate when using Neumann rather than Dirichlet conditions, and also with respect to the structure of the spectral element mesh.

Convergence tests have been carried out for $-\Delta u+u=f$ in the domain Ω, with Dirichlet/Neumann or mixed Dirichlet-Neumann boundary conditions. To this end we have again used the analytical exact solution, u_{exact}, introduced for the single triangle tests, but computations have also been carried out with "less artificial" source term and boundary conditions. As shown in Fig. 3, two different domains have been considered. The first one, $\Omega=(0,10)^2$, corresponds to a Cartesian geometry and so may be discretized with a structured regular mesh, whereas the second one shows a square hole, so that an unstructured mesh is required. For the structured mesh two coarser and one finer versions of this mesh have also been considered. Note that despite the weak number of elements of the mesh, the number of degree of freedom may be important, as shown in Table 2.

Results are provided for different multi-grid approximations, $MG(N_c,\cdots,N_f)$. As for the single triangle test, the algorithm is the one detailed in Fig. 1. We have varied:

- the number of grid-levels, *e.g.*, $MG(6,12)$, $MG(3,6,12)$ and $MG(1,3,6,12)$;
- the polynomial approximation degree at the fine grid level, *e.g.*, $MG(3,6,12)$ and $MG(3,9,18)$;
- the number of spectral elements.

Comparisons with the (single grid) standard Conjugate-Gradient (CG) solver are provided. Note that we do not use a preconditioned CG approach which certainly would be

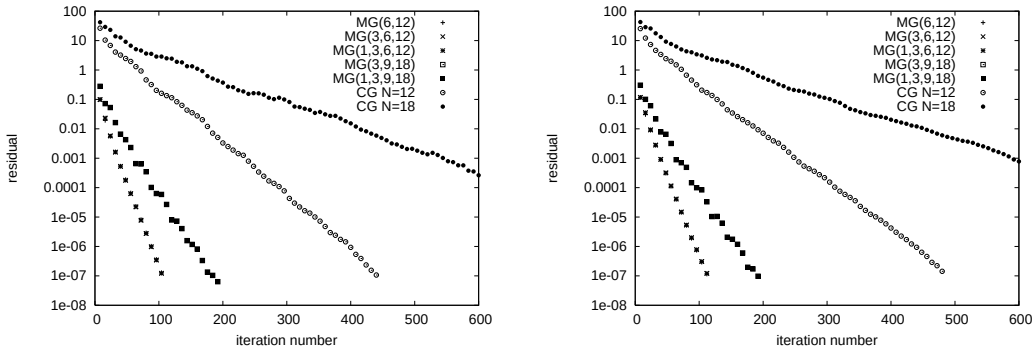

Figure 4: Dirichlet problem: Convergence histories towards the analytical solution with the structured (left) and non-structured (right) meshes. One point each V-cycle (or one point each 8 CG iterations).

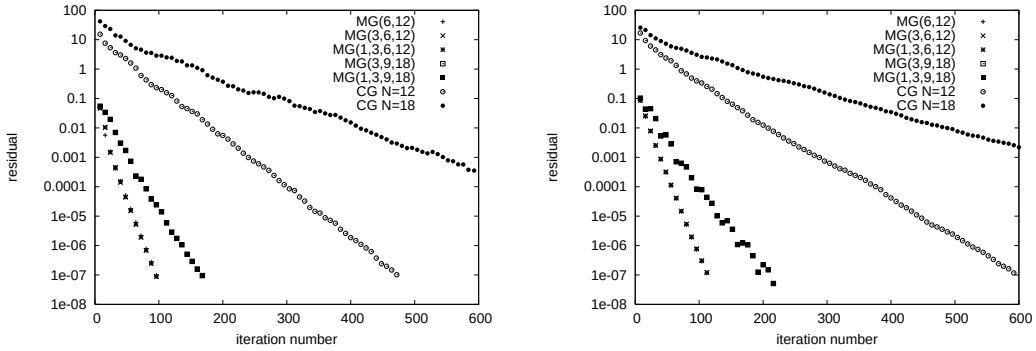

Figure 5: Neumann problem: Convergence histories towards the analytical solution with the structured (left) and non-structured (right) meshes. One point each V-cycle (or one point each 8 CG iterations).

more efficient. The CG results are here only given as reference ones.

In Fig. 4 we compare convergence histories obtained for the Dirichlet problem, when the boundary conditions and the source term correspond to the exact solution. For the plot at left, the domain is Cartesian and the mesh is structured, whereas at right one has the complex domain and the unstructured mesh. The variations of the max norm of the residual are plotted versus the iteration number at the fine grid level, which require the main part of the CPU time. Each point corresponds to a V-cycle or to 8 CG iterations, since at each grid level one has 8 GS iterations with the multigrid method.

Similar results are given for the Neumann problem in Fig. 5.

Results obtained for Dirichlet-Neumann problems and the unstructured mesh are shown in Fig. 6. The Neumann condition holds at the inner boundary whereas a Dirichlet condition is applied at the outer. At left we have again used the analytical solution to fix the source term and the boundary values. At right the following less artificial problem has been considered: no source term, *i.e.*, $f=0$, Neumann condition $\partial_n u=1$ at the inner boundary and Dirichlet condition $u=0$ at the outer boundary.

It is also of interest to point out the influence of the number of elements. This can

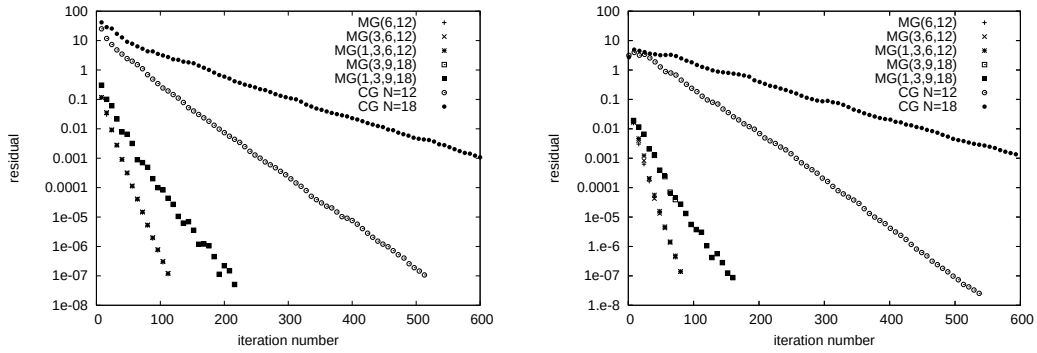

Figure 6: Dirichlet-Neumann problem (non-structured mesh): Convergence histories towards the analytical solution (left) and with the more realistic problem (right).

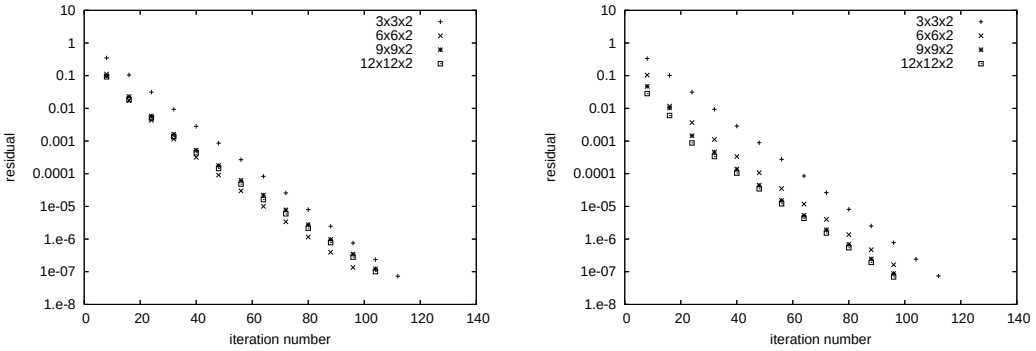

Figure 7: Dirichlet (left) and Neumann (right) problems with four different structured meshes for $MG(3,6,12)$.

easily be done with the structured mesh. In Fig. 7 convergence histories are presented for both the Dirichlet and Neumann problems, for different spectral element discretizations. Clearly, the curves of Fig. 7 are quasi-parallel, *i.e.*, the convergence rates are nearly independent on the number of elements.

From these numerical tests one can state: For the considered elliptic problems the convergence rates depend essentially on the polynomial approximation degree N_f at the fine-grid level.

Thus, for N_f given similar convergence rates are obtained for:

- similar structured and non-structured meshes: The convergence rates do not deteriorate when going from the structured to the non-structured mesh;
- Dirichlet, Neumann or Dirichlet-Neumann boundary conditions;
- different numbers of spectral elements;
- different numbers of grid-levels: A direct solve at the coarsest grid-level $N_c = 1$ is then possible, thus providing a natural coarse solver.

To be more precise, one can provide such convergence rates. They are generally computed per V-cycle, but to compare MG computations using different numbers of smooth-

ings, one can prefer to express them per iteration at the fine grid level. With ρ for the convergence rate and $\|r_l\|$ for the max norm of the residual at iteration l:

$$\|r_l\| \approx \rho^l \|r_0\|, \quad \log\|r_l\| \approx l\log\rho + C. \tag{4.2}$$

Moreover, the scaling of the number of iterations at the fine grid level with respect to the fine grid polynomial degree N_f can also be provided. For the CG method, it is well known that the number of iterations scales like the square root of the condition number, say κ, of the system matrix. In the case of the Fekete-Gauss approximation $\kappa = \mathcal{O}(N^4)$, so that the number of iterations is $\mathcal{O}(N^2)$, and indeed one can check, see Figs. 4-6, that the ratio of the slopes of the curves corresponding for CG to $N_f = 12$ and $N_f = 18$ differ approximately by a factor $2.25 = (18/12)^2$. For MG, one observes that the number of iterations is $\mathcal{O}(N^\alpha)$, with $\alpha < 2$.

Table 3: Convergence rates for $N_f = 12$ and $N_f = 18$ and associated scaling coefficient for the different test-cases of Fig. 6 (D. 1/D. 2 for the graph at left/right), Fig. 7 (N. 1/N. 2) and Fig. 8 (D.N. 1/D.N. 2). Case D.N. 3 makes use of the $T-D$ strategy and D.N. 4 of 4 GS smoothings per grid level.

	D. 1	D. 2	N. 1	N. 2	D.N. 1	D.N. 2	D.N. 3	D.N. 4
ρ_{12}	0.879	0.877	0.874	0.881	0.879	0.860	0.880	0.880
ρ_{18}	0.925	0.922	0.921	0.936	0.931	0.923	0.932	0.931
α	1.24	1.17	1.22	1.60	1.46	1.56	1.48	1.44

Quantitative results are given in Table 3. For the cases that have been considered we present, for $N_f = 12$ and $N_f = 18$, the convergence ratio, ρ_{12} and ρ_{18}, respectively, and the scaling coefficient α. Results are also provided for the Dirichlet-Neumann test case, with analytical solution and unstructured mesh, using the *T-D* strategy, *i.e.*, the system matrix is not set up by aggregation but directly, see case D.N. 3. One can observes that the convergence rates for *T-D* and *T-A* are very similar and so that the results obtained for the single triangle transfer well to the full mesh. Another result, case D.N. 4, corresponds to the Dirichlet-Neumann problem, but using 4 GS smoothings at each level rather than 8. Here again one observes that the convergence rate per iteration is nearly the same, whereas of course it is the square root per V-cycle. All calculations have been carried out without preconditioning of the GS smoother, so that one may expect to decrease the value of the scaling factor α. Note that the values of this parameter in Table 3 are approximate, since resulting from computations carried out for only two different values of N_f.

At the end, the multigrid approach intends to diminish the computational cost, which essentially corresponds to the iterative resolution. A crude operation count shows that the number of elemental operations required by the GS smoothings at the fine grid level scales like $K_e N_f^4$, where K_e is the number of spectral elements. If the number of GS smoothings is $\mathcal{O}(N^\alpha)$, then one can expect a $\mathcal{O}(K_e N_f^{4+\alpha})$ computational cost. To be more precise we give in Fig. 8 the variations of the CPU time required to decrease the residual by a factor 10^{-6}, when varying K_e or N_f, *i.e.*, the number of degrees of freedom

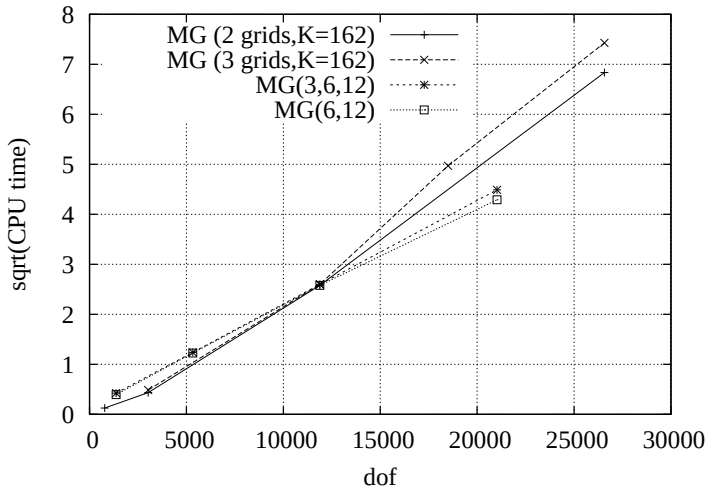

Figure 8: Dirichlet problem: Square root of CPU time versus the number of degrees of freedom, for different MG approximations (MG(3,6), MG(6,12), MG(9,18) and MG(1,3,6), MG(3,6,12), MG(3,9,18)) on a $9\times9\times2$ mesh and of $MG(3,6,12)$ and $MG(6,12)$ on different meshes ($3\times3\times2$, $6\times6\times2$, $9\times9\times2$, $12\times12\times2$).

$dof=\mathcal{O}(K_eN_f^2)$. The results are presented for different MG combinations, based on 2 and 3 grid levels. As expected, (i) increasing the polynomial approximation degree N_f is more time consuming than increasing the number of elements K_e and (ii) the 3 level computations are only slightly more costly than the 2 level ones. These CPU time measurements, carried out on a SGI workstation, are however mainly governed by hardware reasons (CPU cache), so that the agreement with the operation count is poor, especially when varying dof by changing the number of spectral elements since a linear variation could be expected. Let us also mention that CG solvers are more costly than MG ones: Thus, for $N_f=12$ we have checked that 8 CG iterations were about twice more time consuming than MG solves based on 8 GS smoothings at each level.

5 Conclusion

Spectral element approximations of elliptic problems generally result in severely ill-conditioned algebraic systems. Thus, when using triangular Fekete-Gauss spectral elements, the condition number shows an $\mathcal{O}(N^4)$ behavior with respect to the total degree N of the polynomial approximation. It is then of interest to develop efficient resolution strategies. Here we have presented a p-multigrid approach for Fekete-Gauss spectral element approximations of elliptic problems.

The p-multigrid method makes use of a single (rough) mesh and it is the degree of the polynomial approximation which is uniformly changed in each mesh element. Its efficiency relies on good choices of the smoother, of the restriction and prolongation operators and of the way used to set up the coarse grid algebraic systems. Essentially, it

has been shown that it was suitable (i) to use the transpose of the natural prolongation operator for the restriction operator, (ii) to set up the coarse grid systems directly, i.e., as the finest one, or by aggregation of the finer ones and (iii) that satisfactory results could be obtained with a standard Gauss-Seidel smoothing. For the Fekete-Gauss *T*SEM, the MG scheme appears scalable with respect to the number of spectral elements and only weakly sensitive to the number of smoothings per grid level. However, by contrast to the 1D case explored in [18, 23] and similarly to the 2D SEM [24], the MG scheme is not scalable with respect to the polynomial approximation degree at the fine grid level.

We have especially focused on the robustness of the method with respect to the mesh and to the boundary condition types: (i) similar results have been obtained for a structured meshing of a square domain and for a fully non-structured mesh of the complex domain which results from the inclusion of a hole inside the square and (ii) no deterioration of the convergence rates have been observed when Neumann conditions are substituted to the Dirichlet conditions. Moreover, the number of V-cycles required to reach a negligible value of the residual is independent of the numbers of levels, thus allowing to use a direct (or CG) solver only at the coarsest level.

References

[1] L. Bos, On certain configurations of points in $\mathbb{R}^n$ which are unisolvent for polynomial interpolation, J. Approx. Theory, 64 (1991), 271-280.
[2] L. Bos, M.A. Taylor and B.A. Wingate, Tensor product Gauss-Lobatto points are Fekete points for the cube, Math. Comp., 70 (2001), 1543-1547.
[3] Briggs, Henson and McCormick, A multigrid tutorial, 2nd Ed., SIAM Publications (2000).
[4] Q. Chen and I. Babuska, Approximate optimal points for polynomial interpolation of real functions in an interval and in a triangle, Methods Appl. Mech. Engrg., 128 (1995), 485-494.
[5] Q. Chen and I. Babuska, The optimal symmetrical points for polynomial interpolation of real functions in a tetrahedron, Comput. Methods Appl. Mech. Engrg., 137 (1996), 89-94.
[6] R. Cools, Advances in multidimensional integration, J. Comput. Appl. Math., 149 (2002), 1-12.
[7] L. Demkowicz, T. Walsh, K. Gerdes and A. Bajer A., 2D hp-adaptative finite element package Fortran 90 implementation (2Dhp90), TICAM Report, 98-14 (1998).
[8] M.O. Deville, P.F. Fischer and E.H. Mund, High-order methods for incompressible flows, Cambridge University Press, 2002.
[9] V. Doléan, R. Pasquetti and F. Rapetti, p-Multigrid for Fekete spectral element method, 17th International Conference on Domain Decomposition Methods, Strob (Austria), 3-7 July 2006. Proc. in LNCSE Num. 60, Springer, Eds U. Langer et al., 485-492, 2007.
[10] M. Dubiner, Spectral methods on triangles and other domains, J. Sci. Comput., 6 (1991), 345-390.
[11] P.F. Fischer and J.W. Lottes, Hybrid Schwarz-multigrid methods for the spectral element method: Extensions to Navier-Stokes, J. Sci. Comput., 6 (2005), 345-390.
[12] H. Heinrichs, Spectral multigrid methods for the reformulated Stokes equations, J. Comput. Phys., 107 (1993), 213-224.
[13] J.S. Hesthaven, From electrostatic to almost optimal nodal sets for polynomial interpolation in a simplex, SIAM J. Numer. Anal., 35 (1998), 655-676.

[14] J.S. Hesthaven and C.H. Teng, Stable spectral methods on tetrahedral elements, SIAM J. Sci. Comput., 21 (2000), 2352-2380.
[15] J.S. Hesthaven and T. Warburton, Nodal high-order methods on unstructured grids, J. Comput. Phys., 181 (2002), 186-221.
[16] G.E. Karniadakis and S.J. Sherwin, Spectral hp Element Methods for CFD, Oxford Univ. Press, London (1999).
[17] K.J. Fidkowski, T.A. Oliver, J. Lu and D.L. Darmofal, *p*-Multigrid solution of high-order discontinuous Galerkin discretizations of compressible Navier-Stokes equations, J. Comput. Phys., 207 (2005), 92-113.
[18] Y. Maday and R. Munoz, Spectral element multigrid. II. Theoretical justification, J. Sci. Comput., 3 (1988), 323-353.
[19] C.R. Nastase and D.J. Mavriplis, High-order discontinuous Galerkin methods using a spectral multigrid approach, AIAA 2005-1268 Paper (2005).
[20] R. Pasquetti and F. Rapetti, Spectral element methods on unstructured meshes: comparisons and recent advances, J. Sci. Comput., 27 (2006), 377-387.
[21] R. Pasquetti, F. Rapetti, L. Pavarino and E. Zampieri, Neumann-Neumann Schur complement methods for Fekete spectral elements, J. Eng. Math., 56(3) (2006), 323-335.
[22] L.F. Pavarino, E. Zampieri, R. Pasquetti and F. Rapetti, Overlapping Schwarz methods for Fekete and Gauss-Lobatto spectral elements, SIAM J. Sci. Comput., 29(3) (2007), 1073-1092.
[23] E.M. Ronquist and A.T. Patera, Spectral element multigrid. 1- Formulation and numerical results, J. Sci. Comput., 2 (1987), 389-405.
[24] E.M. Ronquist, Optimal spectral element methods for the unsteady three-dimensional incompressible Navier-Stokes equations, Ph.D. Thesis (1988).
[25] A.H. Stroud and D. Secrest, Gaussian quadrature formulas, Prentice Hall (1966).
[26] A.H. Stroud, Approximate calculations of multiple integrals, Prentice Hall (1971).
[27] M.A. Taylor, B.A. Wingate and R.E. Vincent, An algorithm for computing Fekete points in the triangle, SIAM J. Numer. Anal., 38 (2000), 1707-1720.
[28] M.A. Taylor and B.A. Wingate, A generalized diagonal mass matrix spectral element method for non-quadrilateral elements, Appl. Numer. Math., 33 (2000), 259-265.
[29] M.A. Taylor, B.A. Wingate and L.P. Bos, A new algorithm for computing multivariate Gauss-like quadrature points, ICOSAHOM 2004 Congress, Brown University (2004).
[30] B.A. Wingate and M.A. Taylor, Performance of numerically computed quadrature points, Appl. Numer. Math., in press.
[31] T. Warburton, L. Pavarino and J.S. Hesthaven, A pseudo-spectral scheme for the incompressible Navier-Stokes equations using unstructured nodal elements, J. Comput. Phys., 164 (2000), 1-21.
[32] P. Wesseling, An Introduction to Multigrid Methods, R.T. Edwards, Inc. (2004).
[33] T.A. Zang, Y.S. Wong and M.Y. Hussaini, Spectral multigrid methods for elliptic equations, J. Comput. Phys., 48 (1982), 485-501.